

# The molecular chaperone TF55

## Assesment of symmetry

Sergio Marco<sup>a</sup>, Dionisio Ureña<sup>b</sup>, José L. Carrascosa<sup>a,\*</sup>, Thomas Waldmann<sup>c</sup>, Jürgen Peters<sup>c</sup>,  
Reiner Hegerl<sup>c</sup>, Günter Pfeifer<sup>c</sup>, Hilde Sack-Kongehl<sup>d</sup>, Wolfgang Baumeister<sup>c</sup>

<sup>a</sup>Centro Nacional de Biotecnología (CSIC), Universidad Autónoma de Madrid, Cantoblanco, 28049 Madrid, Spain

<sup>b</sup>Centro de Biología Molecular (CSIC-UAM), Universidad Autónoma de Madrid, Madrid, Spain

<sup>c</sup>Max-Planck-Institut für Biochemie, D-82152 Martinsried, Germany

<sup>d</sup>Fritz-Haber-Institut of the Max-Planck-Gesellschaft, Berlin, Germany

Received 3 January 1994; revised version received 3 February 1994

### Abstract

TF55-like factor from *Sulfolobus solfataricus* was purified to homogeneity and analyzed by electron microscopy and image analysis to determine the symmetries of these particles. Three different procedures were used to analyze the electron micrographs: (1) fuzzy-set based classification of the particles according to their rotational power spectra; (2) multivariate statistical analysis based on singular value decomposition; (3) circular harmonic analysis. Averages obtained from the three methods show unequivocally that the TF55-like complex presents a 9-fold symmetry.

**Key words:** Molecular chaperone; Rotational symmetry; Thermophilic factor (TF55)

### 1. Introduction

Molecular chaperones are proteins which assist other proteins in folding, translocation, and assembly [1,2]. They are common in prokaryotes as well as in eukaryotes, and can be classified according to the molecular mass of the constituent polypeptides and to sequence similarities. They fall into three major families: hsp60, hsp70 and hsp90; all of them are constitutively expressed in cells and they are specifically induced by cellular stress (for a recent review see [3]).

The thermophilic factor 55 (TF55) which is related to the acquisition of thermotolerance in *Sulfolobus shibatae*, has been shown to interact with unfolded proteins, thus preventing their aggregation, and to possess ATPase activity [4]. TF55 has a high degree of sequence homology to the eukaryotic t-complex polypeptide 1 (TCP1), which is part of a heteromeric complex [5] that plays an important role in tubulin assembly, both in vivo and in vitro, and in the folding of actin (for a recent review see [6]). Furthermore, the TCP1 complex and TF55 have conspicuous structural similarities: both are grossly cylinder-shaped double-ring structures; when viewed along the cylinder axis ('end-on') they exhibit

radial symmetry. In the case of TF55, most of the particles show 9-fold symmetry, 'but some 8-fold symmetrical complexes are also seen' [4]. Similarly, rings containing 8 or 9 subunits have been described for the TCP1-containing complex [7].

A large number of thermophilic archaeobacteria possess an ATPase complex, the 'thermosome', which accumulates upon heat shock, and is structurally very similar to the TF55 and the TCP1 complex [8]. A detailed study of the thermosome from *Pyrodicticum occultum* has shown that it is made of two rings comprising 8 subunits each, which enclose a large central cavity [9]. Such a cavity is a feature reminiscent of the hsp60 GroEL [10]. Based on sequence data, morphological similarities, and function, thermosomes, TF55 and the TCP1-containing complex have been proposed to be members of a new type of molecular chaperone, related to the hsp60-chaperonin group [8,9].

In an attempt to extend our knowledge about the structure of this molecular chaperone and to settle the uncertainty with regard to its symmetry, we have studied a TF55-like protein from *Sulfolobus solfataricus*, like *Sulfolobus shibatae* a thermophilic sulfur-metabolizing archaeobacterium. A single polypeptide species with an apparent molecular weight of 60 kDa assembles to form a complex with a molecular weight of approx. 1000 kDa. Its structure, as determined by electron microscopy in conjunction with image analysis is, at a resolution of

\*Corresponding author. Fax: (34) (1) 585 4506;  
E-mail: JLCARRASCOSA@SAMBA.CNB.UAM.ES

2 nm, indistinguishable from the TF55 complex of *S. shibatae*. We have scrutinized highly purified preparations of this protein with regard to the coexistence of different oligomeric forms and using three different strategies for the analysis of individual particles, we have determined the genuine symmetry of this molecular complex.

## 2. Materials and methods

### 2.1. Preparation of the protein complex

*Sulfolobus solfataricus* (DSM 1616 (MT4)) was grown at 85°C in a 100-liter polypropylene vessel (with controlled stirring, temperature and air bubbling) in a medium containing yeast extract (1 g/l), caseaminoacids (1 g/l),  $H_2PO_4K$  (3.1 g/l),  $SO_4(NO_3)_2$  (2.5 g/l),  $MgSO_4 \cdot 7H_2O$  (0.2 g/l), and  $CaCl_2 \cdot 2H_2O$ , adjusted to pH 2.5, and collected in the early logarithmic phase ( $OD = 0.4$  at 600 nm). 1.5 g of frozen cells were rehydrated in 3 ml 10 mM Tris-HCl, pH 7.7, 5 mM  $MgCl_2$ , 100  $\mu$ g/ml DNase II and broken with 6 g of glass beads in a Vibrogen cell mill. To remove the glass-beads from cellular material the mixture was centrifuged at  $2000 \times g$ , for 1 min and the sediment once washed with buffer and centrifuged again to recover cell protein in the supernatant. Subsequently, the combined supernatants were centrifuged at  $10,000 \times g$  for 5 min, followed by centrifugation at  $30,000 \times g$  for 20 min at 4°C. The supernatant was directly applied to a Fractogel EMD TMAE-650 (S) tentacle anion-exchange column (Merck), equilibrated with 20 mM Tris-HCl, pH 7.7, containing 1 mM  $NaN_3$ . The column (30 cm long, 1 cm diameter) was developed with a linear gradient ranging from 80 mM to 1 M sodium chloride in the running buffer over 2 h with a flow rate of 0.5 ml/min. Fractions of 1 ml, containing the complex, were loaded on a linear density gradient of 10–30% (w/v) sucrose in 50 mM Tris-HCl (pH 7.7), 200 mM NaCl, 2 mM  $NaN_3$ . Centrifugation was done at 38,000 rpm in a Beckman SW41 rotor (Beckman L8 ultracentrifuge) for 15 h at 4°C. Fractions of 0.5 ml containing the complex were loaded on a Superose 6 gel filtration column (15 cm long, 1 cm diameter) (Pharmacia) equilibrated with 5 mM HEPES, pH 7.3, 200 mM NaCl and eluted at a flow rate of 0.5 ml/min. All purification steps were monitored by means of electron microscopy and, additionally, by 10% SDS-polyacrylamide gels using a Tris/Tricine buffer system [11]. Proteins were stained with colloidal Coomassie blue [12].

### 2.2. Electron microscopy and image processing

For electron microscopy, the particles were negatively stained on the grid with 2% uranyl acetate. Using a Philips CM12 operated in the low-dose mode at 120 kV, micrographs were recorded at a primary magnification of 33,600 times. Five non-overlapping areas from one micrograph, selected on grounds of particle coverage, even staining, and focus setting, were digitized, using an Eikonix 1412 camera system. Each of these pictures was represented by  $2048 \times 2048$  pixels with a pixel size of 15  $\mu$ m, corresponding to 0.446 nm at the specimen level. In order to remove high-frequency noise as well as long-range contrast variations, the images were band-pass filtered in Fourier space within space frequency limits of  $(1.4 \text{ nm})^{-1}$  and  $(20 \text{ nm})^{-1}$ . From these images small subframes with  $64 \times 64$  pixels were extracted, each one containing an individual particle in the end-on orientation.

The analysis of this data set was performed independently in three different laboratories (Centro Nacional de Biotecnología, Madrid; Max-Planck-Institut für Biochemie, Martinsried; Fritz-Haber-Institut der Max-Planck-Gesellschaft, Berlin) using different approaches and software packages.

**Procedure (1).** All particles were translationally aligned using a synthetic ring-like pattern as reference. Rotational power spectra [13] were obtained for a significant area of the specimen including the periphery of the particle. Fuzzy-set classification methods were applied using the k-nearest-neighbour (KNN) algorithm [14,15] with a fuzzy parameter of 1.5 and threshold decision of 0.8 in the pertinence function. Each particle was assigned to a class of symmetry, according to its prevailing contribution to 8- or 9-fold symmetry. Orientational alignment was performed within each class as well as with the whole data set using a free pattern alignment algorithm [16]; finally averages were calculated.

**Procedure (2).** The particles were aligned translationally using an iterative procedure which created a new reference upon each cycle by summing up all aligned images. The translationally aligned images were subjected to a multivariate statistical analysis based on singular value decomposition. The resulting non-trivial eigenimages reveal all important features of the image set, including all rotational variations. If there is a predominant  $n$ -fold symmetry axis, a pair of eigenimages with nearly the same size of the corresponding eigenfactors should appear. Both images show basically the same pattern with a  $n$ -fold axis but rotated with respect to each other by an angle of  $\pi/2n$ . Any arbitrary rotation of this pattern can be produced by an adequate linear superposition of these eigenimages. As a consequence, such a pair indicates the existence of an  $n$ -fold axis prior to any rotational alignment which may be biased due to an arbitrarily chosen reference [17]. After classification of all pictures with respect to the set of significant eigenimages, rotational alignment and subsequent averaging was performed for each class separately.

**Procedure (3).** The third approach is a circular harmonic analysis as described by Kunath and Sack-Kongehl [18]. This technique includes classification, rotational alignment, and averaging, but these steps are performed with the circular harmonic components of the images instead of using the images themselves. The procedure was applied subsequent to the translational alignment described in the second procedure.

## 3. Results and discussion

The purification protocol described in section 2 yielded a highly purified preparation of the TF55-like particle with an apparent molecular weight of approx. 1000 kDa (as deduced from the elution volume in gel filtration using molecular weight standards), and composed of a single polypeptide species of approx. 60 kDa (Fig. 1). When this fraction was examined by electron microscopy, a uniform field of particles was seen, predominantly exhibiting a ring-shaped structure (Fig. 2). Only very few particles show a different aspect, either due to a different orientation of the cylinder-shaped particle ('side-on' orientation) or due to some kind of distort-

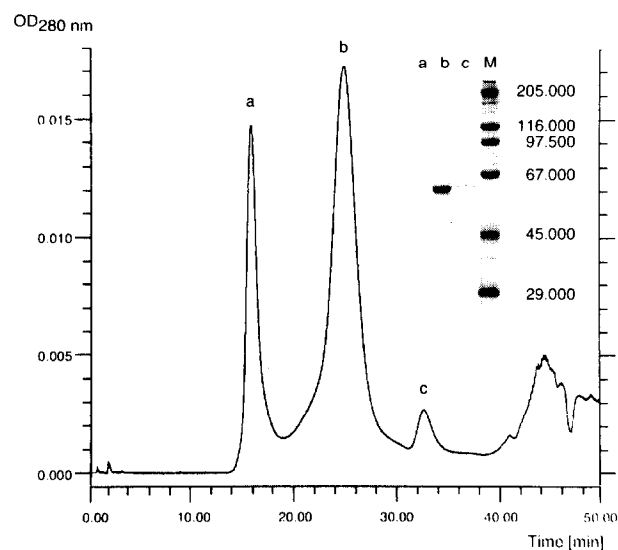


Fig. 1. Superose 6 gel filtration chromatography of a sucrose gradient fraction containing the protein complex and SDS-PAGE. The native complex eluted after 25 min (peak b). Between 5 and 10% of the native complex disassembled into its subunits which were eluted after approx. 32.2 min (peak c). In peak a no protein was detected by SDS-PAGE.

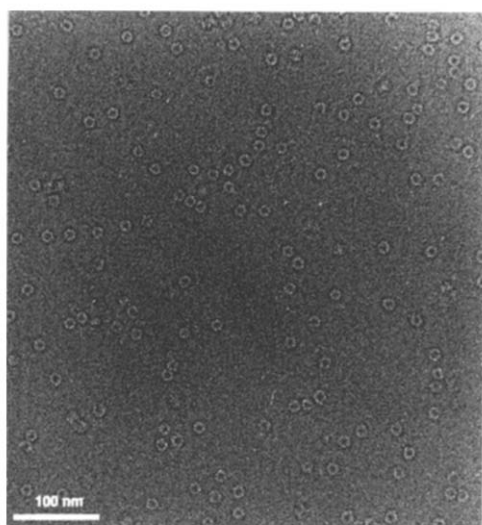


Fig. 2. Subframe of the electron micrograph used for image processing. Most particles show a ring-shaped structure corresponding to the end-on view of a roughly cylinder-shaped complex. Bar = 100 nm.

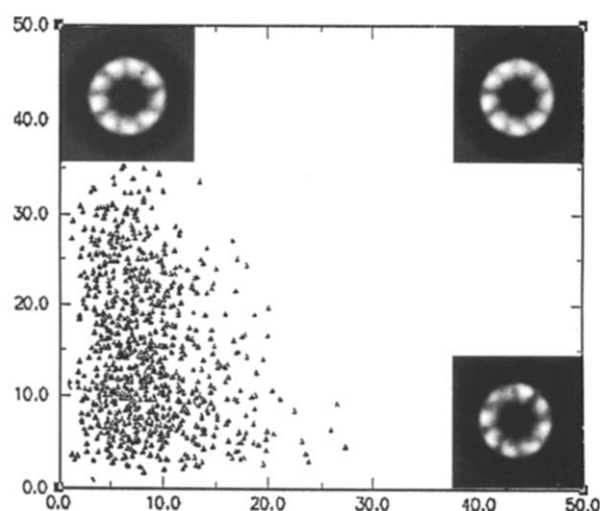


Fig. 3. TF55 views clustered by a supervised fuzzy-set method. Values along the Y and X axis represent percentage of the total energy for the 9th and 8th order harmonics, respectively. The average images for the 9- and 8-fold symmetry particles are shown in the top left and bottom right corners, respectively. The average image for the whole population is shown in the top right corner.

tion. A total of 921 individual images of the complex in the end-on view orientation were extracted from the digitized micrograph and subjected to the three image processing procedures described in section 2.

With the first approach, averages were calculated separately for each class corresponding to 8- or 9-fold symmetry (Fig. 3). As expected, the average of the class with 9-fold symmetry shows a pattern with 9 maxima regu-

larly arranged on a circle. However, also the average of particles assigned to the small class with 8-fold symmetry reveals 9 maxima, though in a more irregular arrangement. Such irregularities may arise from deviations from perfect 'end-on' orientation or from preparation induced distortions. Their contribution to 8-fold symmetry in the rotational power spectrum analysis may be understood

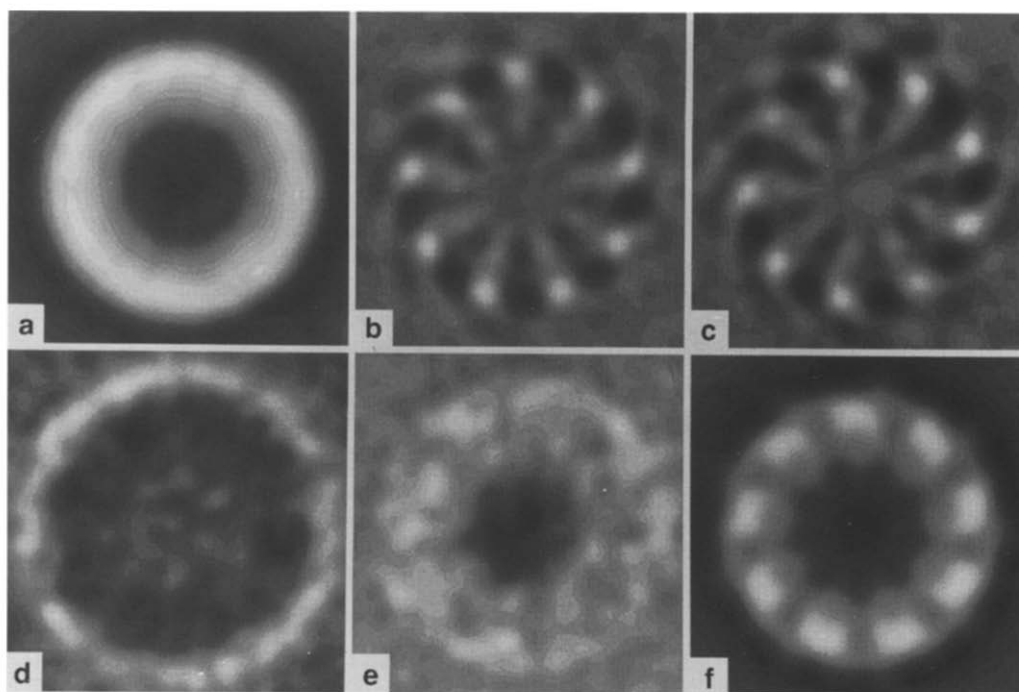


Fig. 4. The first five eigenimages, (a) – (e), obtained by multivariate statistical analysis of 921 particles which were aligned translationally but not rotationally. The pair (b) and (c) of eigenimages indicates the predominance of a 9-fold symmetry axis. (f) shows the total average after rotational alignment.

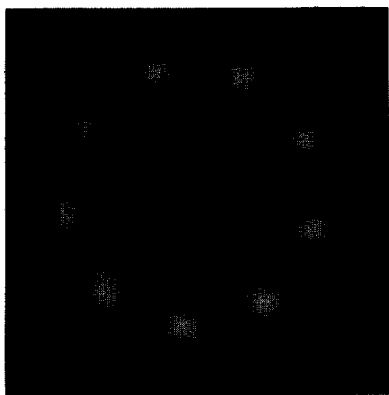


Fig. 5. Total average obtained by circular harmonic analysis.

as a consequence of the random variations of the angular distance between neighbouring subunits. The average of the whole set of particles is shown in Fig. 3, clearly revealing a particle with 9 subunits.

The second approach based on multivariate statistical analysis yields a set of eigenimages which represents the main features underlying the whole set of particles. In other words, each individual image of a particle can be composed by an adequate linear superposition of these eigenimages. The eigenvalue belonging to each eigenimage indicates the contribution of the corresponding feature to the total variance within the whole particle set. The first eigenimage of the actual set is a simple ring which represents the average of all rotationally unaligned particles (Fig. 4a). The second and third eigenimage, representing 2.38 and 2.18% of the total variance, show almost identical patterns with a clear 9-fold symmetry (Fig. 4b and 4c). They differ by a rotation of about 10 degree, corresponding to  $\pi/(2n)$  with  $n = 9$ . As pointed out in section 2, this pair of eigenimages indicates clearly the predominance of a 9-fold axis. The next eigenimage (Fig. 4d) with a much lower weight of 1.51% probably reflects variations in size or stain distribution. The last one shown (Fig. 4e) with a weight of 1.30% gives a weak hint as to 8-fold symmetry; however, subsequent rotational alignment, classification, and averaging did not reveal any subset of particles with 8-fold symmetry. For the appearance of this feature the same reasons as mentioned in the preceding paragraph may be responsible. Fig. 4f shows the total average after rotational alignment.

This finding was corroborated by the circular harmonic analysis. The final average is shown in Fig. 5, again demonstrating a particle with 9-fold symmetry. The detailed analysis, not presented here, has rendered the harmonic component of order 8 to be the second highest in weight (ignoring the zero order component

which is of no significance). The corresponding Q-factor, however, is below the limit of 0.6 which rejects this component as not being significant and makes the presence of a class with 8-fold symmetry unlikely. For the definition and use of the Q-factor, see Kunath and Sack-Kongehl [18].

In summary, image analysis of electron micrographs of highly purified preparations of the TF55-like complex from *Sulfolobus solfataricus* unequivocally reveals the existence of 9-fold symmetry. There is no evidence for the existence of a subset of particles with genuine 8-fold symmetry. This is in contrast to the related thermosome complex from *Pyrodicticum occultum* which, according to the same criterion, has (pseudo-) 8-fold symmetry. Unlike the *Sulfolobus* TF55 complex which is made of one type of subunit only, the thermosome is composed of two different, though homologous, (56 and 59 kDa) subunits.

**Acknowledgements:** This work was partly supported by grants PB91-0109 from the Dirección General de Investigación Científica y Técnica to J.L.C. and the Deutsche Forschungsgemeinschaft (Ty2/4-1).

## References

- [1] Ellis, R.J. and van der Vies, S.M. (1991) *Annu. Rev. Biochem.* 60, 321–347.
- [2] Hendrick, J.P. and Hartl, F.-U. (1993) *Annu. Rev. Biochem.* 62, 349–384.
- [3] Gething, M.-J. and Sambrook, J. (1992) *Nature* 355, 33–55.
- [4] Trent, J.D., Nimmesgern, E., Wall, J.S., Hartl, F.U. and Horwich, A.L. (1991) *Nature* 354, 490–493.
- [5] Flydman, J., Nimmesgern, E., Erdjument-Bromage, H., Wall, J.S., Tempst, P. and Hartl, F.U. (1992) *EMBO J.* 11, 4767–4778.
- [6] Nelson, R.J. and Craigh, E.A. (1992) *Curr. Biol.* 2, 487–489.
- [7] Lewis, V.A., Hynes, G.M., Zheng, D., Saibil, H. and Willison, K. (1992) *Nature* 358, 249–252.
- [8] Phipps, B.M., Hoffmann, A., Stetter, K.O. and Baumeister, W. (1991) *EMBO J.* 10, 1711–1722.
- [9] Phipps, B.M., Typke, D., Hegerl, R., Volker, S., Hoffmann, A., Stetter, K.O. and Baumeister, W. (1993) *Nature* 361, 475–477.
- [10] Carrascosa, J.L., Abella, G., Marco, S. and Carazo, J.M. (1990) *J. Struct. Biol.* 104, 2–8.
- [11] Schagger, H. and von Jagow, G. (1987) *Anal. Biochem.* 166, 369–379.
- [12] Neuhoff, V., Arold, N., Taube, D. and Ehrhardt, W. (1988) *Electrophoresis* 9, 255–262.
- [13] Crowther, R.A. and Amos, L.A. (1971) *J. Mol. Biol.* 60, 123–130.
- [14] Bezdek, J.C., Chmah, S.K. and Leep, D. (1984) *Fuzzy Sets Syst.* 18, 237–256.
- [15] Carazo, J.M., Rivera, F.F., Zapata, E.L., Radermacher, M. and Frank, J. (1990) *J. Microsc.* 157, 187–203.
- [16] Penzeck, P., Radermacher, M. and Frank, J. (1992) *Ultramicroscopy* 40, 1123–1138.
- [17] Dube, P., Tavares, P., Lurz, R. and van Heel, M. (1993) *EMBO J.* 12, 1303–1309.
- [18] Kunath, W. and Sack-Kongehl, H. (1989) *Ultramicroscopy* 27, 171–184.